Supporting Information

Low-Power Filamentary Memristor Crossbar Array Enabled by Cubic α-Phase Stabilized Mixed-Cation Lead Halide Perovskites

In Hyuk Im[†, 1], Ji Hyun Baek[†, 1], Do Yeon Heo[†, 2, 3], Sung Hyuk Park[1], Sohyeon Park[1], Seung Ju Kim[1, 4], Jae Young Kim[1], Youngmin Kim[1], Yoon Jung Lee[1, 5], Kyung Ju Kwak[1], Hyeon Ji Lee[1], Soo Young Kim[, 2], and Ho Won Jang*[, 1, 6]*

[†] These authors contributed equally.

I. H. Im[†], J. H. Baek[†], S. H. Park, S. Park, S. J. Kim, J. Y. Kim, Y. Kim, Y.J. Lee, K. J. Kwak, H. J. Lee, Prof. H. W. Jang
[1] Department of Materials Science and Engineering
Research Institute of Advanced Materials
Seoul National University
Seoul 08826, Republic of Korea
E-mail: hwjang@snu.ac.kr

D. Y. Heo[†], Prof. S. Y. Kim
[2] Department of Materials Science and Engineering
Korea University
Seoul 02841, Republic of Korea
Email: sooyoungkim@korea.ac.kr

D. Y. Heo[†]
[3] Hydrogen Ion Materials Group
National Institute for Materials Science
Tsukuba, 305-0044, Japan

S. J. Kim
[4] Department of Electrical and Computer Engineering
University of Southern California
Los Angeles, CA 90089, USA

Y. J. Lee
[5] School of Electrical Engineering,
Kookmin University,
Seoul 02707, South Korea

Prof. H. W. Jang
[6] Advanced Institute of Convergence Technology
Seoul National University
Suwon 16229, Republic of Korea
Email: hwjang@snu.ac.kr

ORCID ID

In hyuk Im: https://orcid.org/0000-0001-7402-5356 (im.inhyuk@snu.ac.kr)

Ji Hyun Baek: https://orcid.org/0000-0002-2538-2354 (sanctumgold@snu.ac.kr)

Do Yeon Heo: https://orcid.org/0000-0002-1610-0343 (HEO.Doyeon@nims.go.jp)

Sung Hyuk Park: https://orcid.org/0000-0003-0105-6025 (sunghyuk.park@snu.ac.kr)

Sohyeon Park: https://orcid.org/0009-0009-3365-1030 (shpark9554@snu.ac.kr)

Seung Ju Kim: https://orcid.org/0000-0001-7402-5356 (seungju.kim@usc.edu)

Jae Young Kim: https://orcid.org/0000-0002-2289-2025 (jy2477.kim@snu.ac.kr)

Youngmin Kim: https://orcid.org/0009-0008-4025-4087 (kyminn21@snu.ac.kr)

Yoon Jung Lee: https://orcid.org/0009-0004-8781-6631 (yoonjung.lee@northwestern.edu)

Kyung Ju Kwak: (kj812@snu.ac.kr)

Hyeon Ji Lee: https://orcid.org/ 0009-0002-3299-4604 (hyeonji617@snu.ac.kr)

Soo Young Kim: https://orcid.org/0000-0002-0685-7991 (sooyoungkim@korea.ac.kr)

Ho Won Jang: https://orcid.org/0000-0002-6952-7359 (hwjang@snu.ac.kr)

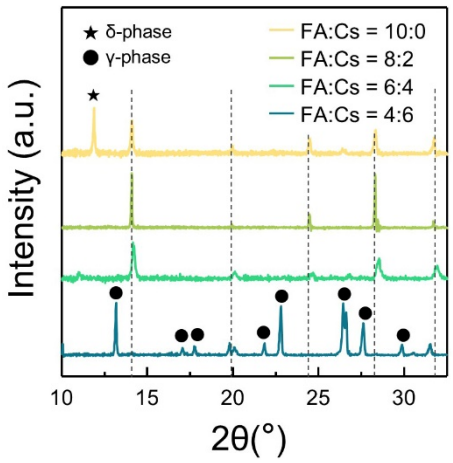

Fig. S1. The XRD results for the $FAPbI_3$, $FA_{0.8}Cs_{0.2}PbI_3$, $FA_{0.6}Cs_{0.4}PbI_3$, and $FA_{0.4}Cs_{0.6}PbI_3$ thin films with NH_4SCN additives.

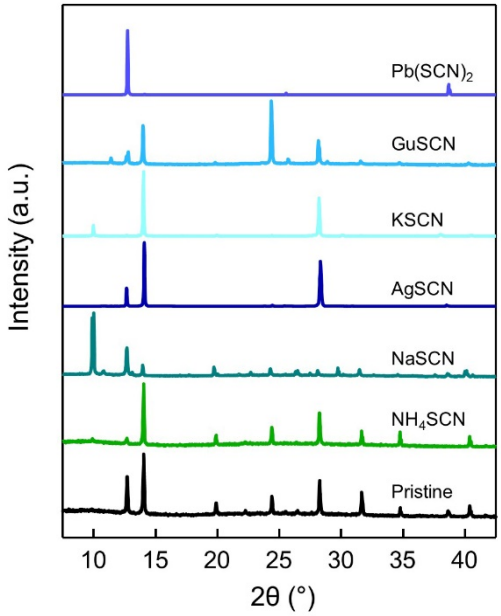

Fig. S2. The XRD results for the FCPI thin films with various *SCN*$^-$-based additives.

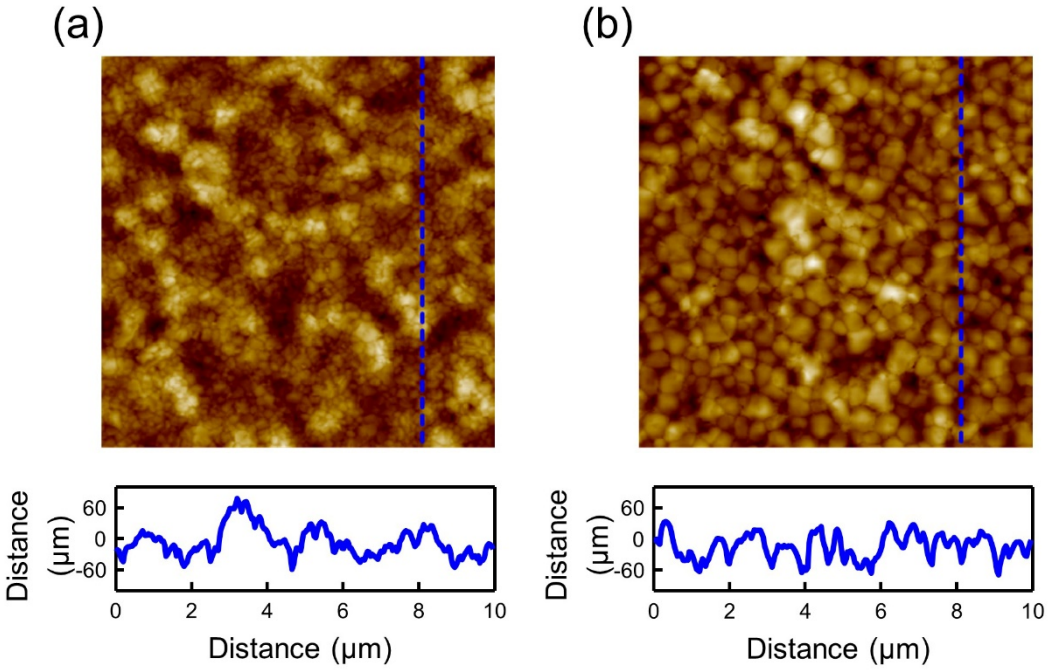

Fig. S3. The AFM image of (a) the pristine FCPI and (b) FCPI-SCN films. The RMS values of roughness are 27.7 nm in the pristine FCPI and 23.8 nm in FCPI-SCN.

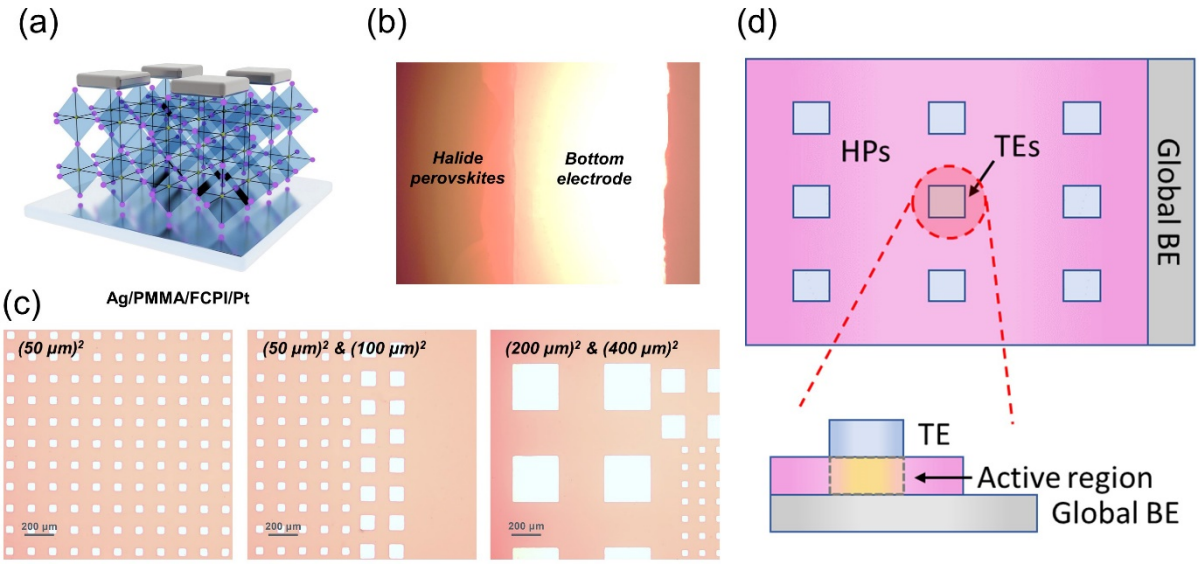

Fig. S4. The optical image of the fabricated device arranged in sandwich structure. (a) Schematic of the devices. (b) Bottom electrode (c) Top electrodes with varying sizes. (d) Illustration of sandwich structure devices.

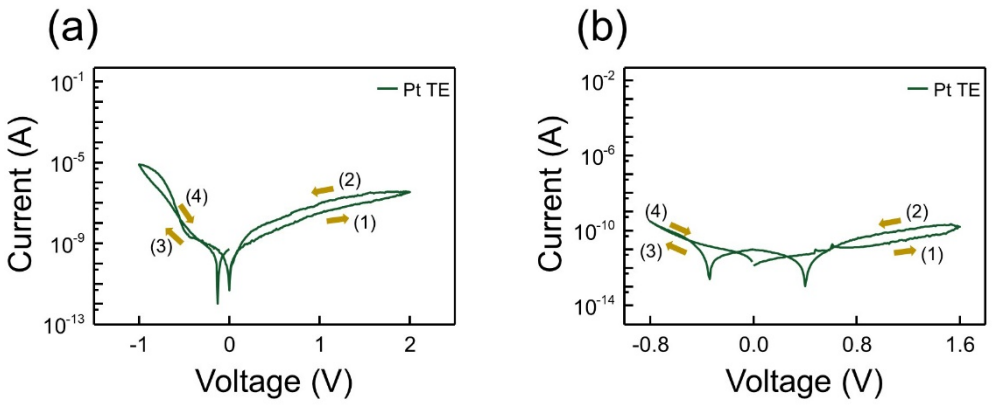

Fig. S5. *I-V* results of the (a) Pt/PMMA/FCPI-SCN/Pt and (b) Pt/PMMA/pristine FCPI/Pt devices, showing no resistive switching response when an Pt TE was adopted instead of Ag TE.

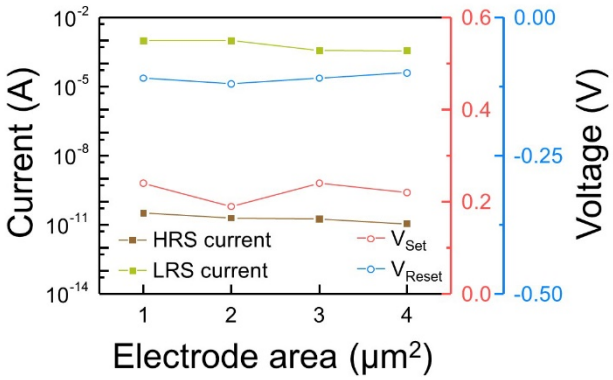

Fig. S6. The electrode size dependence of the V_{SET}, V_{RESET}, and the current of HRS and LRS in the FCPI-SCN devices with varying the electrode sizes, ranging from (50 μm)^2 to (400 μm)^2. The electrical properties are area-independent.

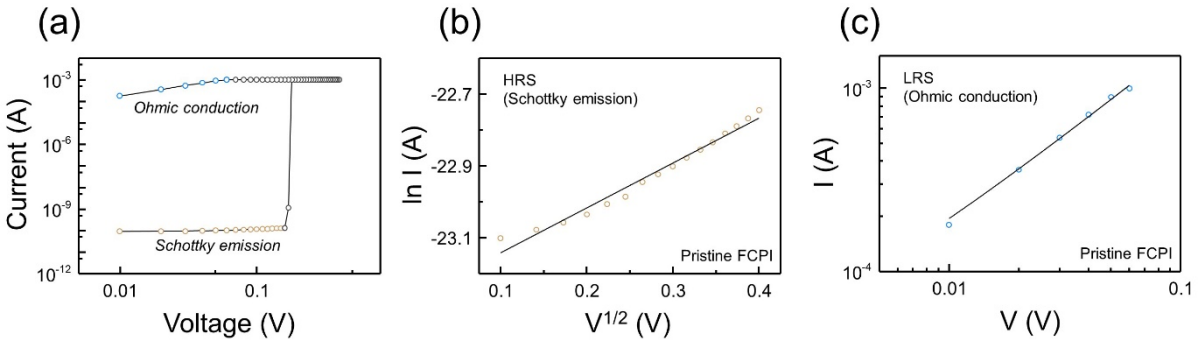

Fig. S7. Analysis of conduction mechanisms in the pristine FCPI device. (a) Double logarithmic plots of *I-V* curves of the pristine FCPI device. (b) $ln\ I - V^{1/2}$ fitting of HRS current before SET, showing Schottky emission. (c) The ohmic conduction region in LRS.

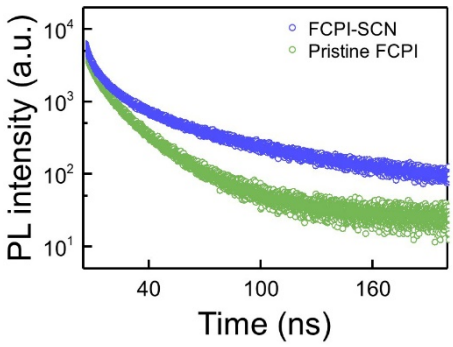

Fig. S8. TR-PL spectra of the pristine FCPI and FCPI-SCN films. The FCPI-SCN film exhibits longer carrier lifetime values (τ_2) of 26.2 ns, compared to the pristine FCPI film displaying 14.1 ns.

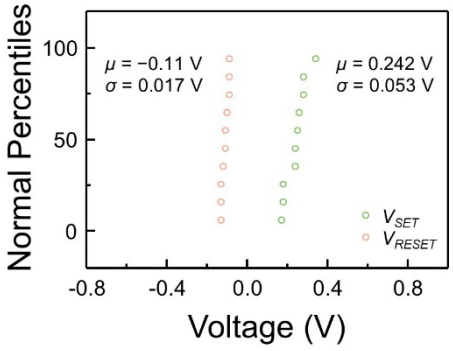

Fig. S9. The cumulative percentiles of V_{SET} and V_{RESET} by 10 sweeps of the FCPI-SCN devices.

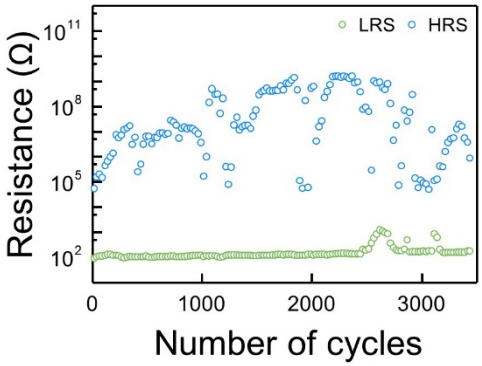

Fig. S10. Endurance result with low amplitude pulses. Endurance test were conducted under pulse train of ±0.2 V (10 μs pulse durations) followed by the read voltage of 0.02 V.

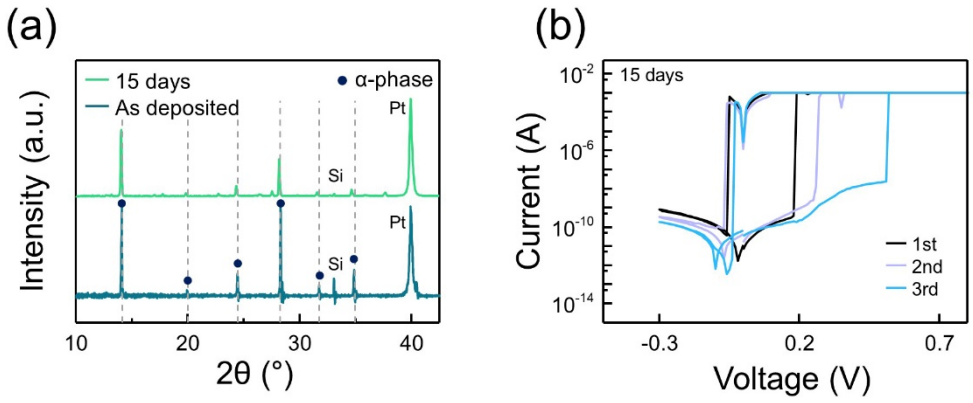

Fig. S11. The XRD patterns of FCPI-SCN film after 15 days in an ambient atmosphere, confirming the retention of the cubic α-phase. (b) *I-V* characteristics of the FCPI-SCN devices after 15 days.

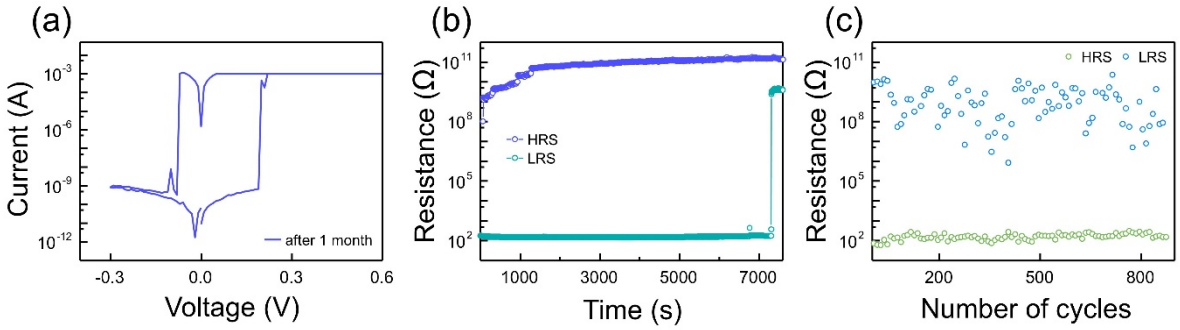

Fig. S12. A longer-duration stability test under ambient air for 30 days. (a) I-V characteristic. (b) Retention time. (c) Endurance cycles.

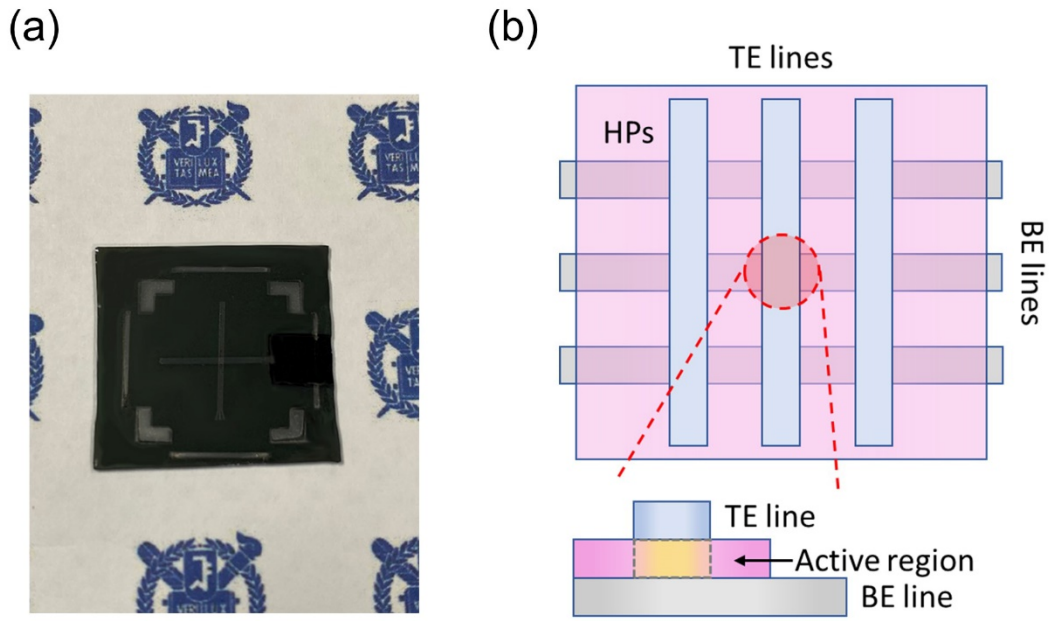

Fig. S13. (a) Full size image and (b) illustration of the 3 × 3 crossbar array.

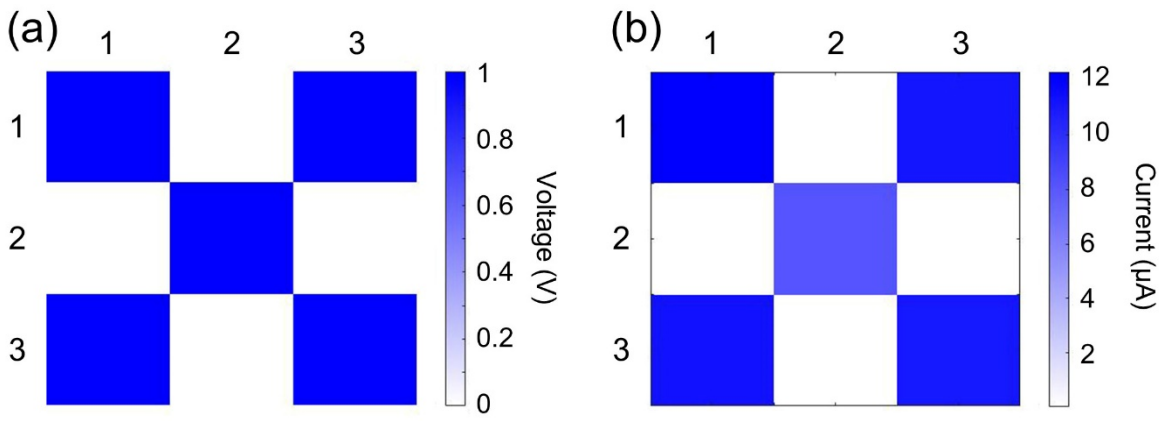

Fig. S14. (a) 3 × 3-pixel voltage input encoded in the shape of an 'X' letter. (b) The current output read out from the programmed 3 × 3 crossbar array.

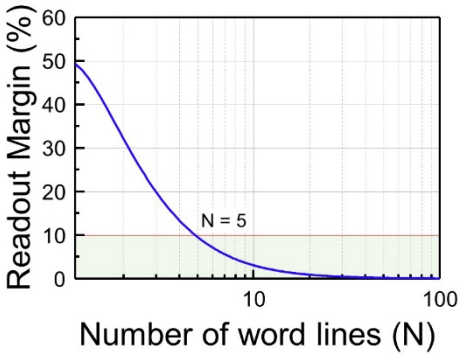

Fig. S15. Calculated readout margin of the FCPI-SCN crossbar array by the Kirchhoff equation, $\frac{\Delta V_{readout}}{V_{pull-up}} = \frac{R_{pull-up}}{\left[R_{LRS} \parallel R_{LRS}^{sneak}\right] + R_{pull-up}} - \frac{R_{pull-up}}{\left[R_{HRS} \parallel R_{LRS}^{sneak}\right] + R_{pull-up}}$, where $\Delta V_{readout}$ is readout margin, $V_{pull\text{-}up}$ is pull-up voltage, $R_{pull\text{-}up}$ is pull-up resistance, and R^{sneak} is the resistances of the neighboring cells. The worst case (all neighboring cells are in LRS) is assumed. At the minimum criterion of a 10% readout margin, the maximum acceptable array size is 5 × 5.